nel agonist that elevates I_{Ca} by a cAMP-independent mechanism (*14*), is illustrated in Fig. 2C. This compound was applied extracellularly during the periods marked "S" in Fig. 2C, and $[Mg^{2+}]_i$ was varied as indicated. Although the effect of (+)202-791 on I_{Ca} decreased somewhat when $[Mg^{2+}]_i$ was increased from 0.3 m*M* to 3.0 m*M*, the decrease was not nearly as large as the decrease that occurred when I_{Ca} was elevated by 3 μ*M* cAMP in the same cell. In nine cells I_{Ca} elevated by (+)202-791 in the presence of 0.3 m*M* $[Mg^{2+}]_i$ was 32 ± 3.7% larger than I_{Ca} in the presence of 3.0 m*M* $[Mg^{2+}]_i$ (Table 1).

The fact that $[Mg^{2+}]_i$ has a small effect on basal I_{Ca} and on I_{Ca} elevated by (+)202-791 suggests that Mg^{2+} may bind to the channel to alter channel gating, but that the Mg^{2+} effect is more pronounced when the channel is phosphorylated. Evidence in support of this suggestion is that the kinetics (primarily the activation kinetics) of I_{Ca} are different in different $[Mg^{2+}]_i$ (Fig. 2D). Alternatively, $[Mg^{2+}]_i$ may regulate protein phosphatase activity. Some phosphatases, particularly protein phosphatase 2C, are known to be regulated by $[Mg^{2+}]$ in this range (*15*).

It is likely that $[Mg^{2+}]_i$ is regulated physiologically because $[Mg^{2+}]_i$ is far from thermodynamic equilibrium in cells, and its concentration changes under a variety of physiological conditions (*8, 11*). For this reason, we propose that $[Mg^{2+}]_i$ may play a role in the physiological regulation of I_{Ca}. Furthermore, the inhibitory effect of $[Mg^{2+}]_i$ on I_{Ca} could explain some of the pathological effects of magnesium deficiency in the heart (*16*). When processes that maintain low $[Ca^{2+}]_i$ are decreased (for example, during ischemia), increases in I_{Ca} produced by loss of $[Mg^{2+}]_i$ could contribute to calcium overload and myocardial damage (*17*).

REFERENCES AND NOTES

1. R. W. Tsien, *Adv. Cyclic Nucleotide Res.* **45**, 363 (1977); *Annu. Rev. Physiol.* **45**, 341 (1983); H. Reuter, *Nature (London)* **301**, 569 (1983); W. Trautwein and D. Pelzer, in *Cardiac Electrophysiology and Arrhythmias*, D. P. Zipes and J. Jalife, Eds. (Grune & Stratton, New York, 1985), p. 31; R. W. Tsien *et al.*, *J. Mol. Cell. Cardiol.* **18**, 691 (1987).
2. A. Noma, H. Kotake, H. Irisawa, *Pfluegers Arch.* **388**, 1 (1980).
3. G. W. Beeler and H. Reuter, *J. Physiol. (London)* **207**, 191 (1970); G. Vassort and O. Rougier, *Pfluegers Arch.* **331**, 191 (1972).
4. R. Fischmeister and H. C. Hartzell, *J. Physiol. (London)* **376**, 183 (1986); H. C. Hartzell and R. Fischmeister, *Nature (London)* **323**, 273 (1986); *Mol. Pharmacol.* **32**, 639 (1987).
5. M. Kameyama, J. Hescheler, G. Mieskes, W. Trautwein, *Pfluegers Arch.* **407**, 461 (1986); J. Hescheler, M. Kameyama, W. Trautwein, *ibid.*, p. 182.
6. P. Horie and H. Irisawa, *Am. J. Physiol.* **253**, H210 (1987); ———, A. Noma, *J. Physiol. (London)* **387**, 251 (1987); C. A. Vandenberg, *Proc. Natl. Acad. Sci. U.S.A.* **84**, 2560 (1987).
7. H. Rubin, *J. Cell. Physiol.* **89**, 613 (1976).
8. P. W. Flatman, *J. Membr. Biol.* **80**, 1 (1984); R. K. Gupta, P. Gupta, R. D. Moore, *Annu. Rev. Biophys. Bioeng.* **13**, 221 (1984).
9. O. P. Hamill, A. Marty, E. Neher, B. Sakmann, F. J. Sigworth, *Pfluegers Arch.* **391**, 85 (1981).
10. R. Godt and B. Lindley, *J. Gen. Physiol.* **80**, 279 (1982). The composition of solutions was calculated to maintain constant 2.6 m*M* magnesium adenosine triphosphate (MgATP), 190 ionic strength, and *p*H 7.15. Stability constants were the same as listed by Godt and Lindley. The compositions of the solutions were as follows (concentrations are m*M*): For 0.3 m*M* $[Mg^{2+}]$: 116.8 CsCl, 10 K · Pipes, 5 K_2EGTA, 3.26 Na_2K_2ATP, 3.04 $MgCl_2$, 5 Na_2 · creatine phosphate, calculated ATP^{-4} was 0.25. For 1.0 m*M* $[Mg^{2+}]$: 118.3 CsCl, 10 K · Pipes, 5 K_2EGTA, 2.80 Na_2K_2ATP, 4.04 $MgCl_2$, 5 Na_2 · creatine phosphate, calculated ATP^{-4} was 0.075. For 3.0 m*M* $[Mg^{2+}]$: 113.5 CsCl, 10 K · Pipes, 5 K_2EGTA, 2.67 Na_2K_2ATP, 6.82 $MgCl_2$, 5 Na_2 · creatine phosphate, calculated ATP^{-4} was 0.025.
11. P. Hess, P. Metzger, R. Weingart, *J. Physiol. (London)* **333**, 173 (1982); J. R. Lopez, L. Alama, C. Caputo, J. Vergara, R. DiPolo, *Biochim. Biophys. Acta* **804**, 1 (1984); L. A. Blatter and J. A. S. McGiugan, *Q. J. Exp. Physiol.* **71**, 467 (1986); S. M. Baylor, W. K. Chandler, M. W. Marshall, *J. Physiol. (London)* **331**, 105 (1982); F. J. Alvarez-Leefmans, S. M. Gamino, F. Giraldez, H. Gonzalez-Serratos, *ibid.* **378**, 461 (1986).
12. R. Fischmeister and H. C. Hartzell, *J. Physiol. (London)* **387**, 453 (1987); J. A. Beavo *et al.*, *Mol. Cell. Endocrinol.* **28**, 387 (1982).
13. R. N. Armstrong, H. Kondo, J. Granot, E. T. Kaiser, A. S. Mildvan, *Biochemistry* **18**, 1230 (1979).
14. S. Kongsamut, T. J. Kamp, R. J. Miller, M. C. Sanguinetti, *Biochem. Biophys. Res. Commun.* **130**, 141 (1985).
15. L. M. Ballou and E. H. Fischer, in *The Enzymes*, P. D. Boyer and E. G. Krebs, Eds. (Academic Press, New York, 1986), vol. 17, p. 311.
16. H. Ebel and T. Gunther, *J. Clin. Chem. Clin. Biochem.* **21**, 249 (1983); M. J. Shattock *et al.*, *J. Am. College Nutr.* **6**, 27 (1987).
17. A. Fleckenstein, in *Calcium and the Heart*, L. Opie, Ed. (Academic Press, New York, 1971), p. 135.
18. H. C. Hartzell and D. Glass, *J. Biol. Chem.* **259**, 15587 (1985).

19. We thank D. Glass for supplying the purified catalytic subunit of cAMP-dependent protein kinase and R. Godt for the computer program for calculating ion composition. Supported by NIH grants HL21195 and HL27385 and a grant-in-aid from the American Heart Association (Georgia Affiliate).

6 October 1987; accepted 31 December 1987

A Fossil Reptile Embryo from the Middle Triassic of the Alps

P. MARTIN SANDER

The first nothosaur (*Neusticosaurus* sp.) embryo, one of the very few fossil embryos known, provides a rare glimpse at reproduction in extinct reptiles. The specimen from the southern Alpine Middle Triassic (about 230 million years ago) was recognized as an embryo in comparison with an exceptionally large and well-understood sample of juvenile and sexed adult *Neusticosaurus* sp. The skeleton shows many embryonic features and may well be the smallest fossil reptile known (body length 51 millimeters). It reached only 22% of mean adult length whereas modern reptiles of this size do not hatch before they reach about 30% of mean adult length. The question of ovipary versus vivipary in pachypleurosaurs is discussed in light of the embryo.

THE ONLY FOSSIL REPTILE EMBRYOS described until now were those of ichthyosaurs (*1*); dinosaur embryos in eggs have recently been found (*2*) but are not yet described. I report the first well-preserved nonichthyosaurian reptile embryo (Fig. 1) of the small pachypleurosaurid nothosaur *Neusticosaurus* sp. (*3*) from the famous Anisian and Ladinian (Middle Triassic, about 230 million years old) Monte San Giorgio bituminous shales (*4, 5*) of southern Switzerland and northern Italy. The specimen possibly is the smallest skeleton of an extinct reptile ever discovered and underscores the exceptional nature of this locality. Its importance is appreciated best in view of how little is known about reproduction in fossil reptiles. Eggs are only known from a few groups such as dinosaurs and turtles (*6, 7*), and embryos only from ichthyosaurs and now pachypleurosaurs.

Neusticosaurus is the most abundant fossil reptile from this locality; about 800 specimens are at the Paleontological Institute and Museum of the University of Zurich (PIMUZ). The mostly complete skeletons belong to two species that are clearly separated stratigraphically. *Neusticosaurus* sp. was a small (adult overall body length 230 to 370 mm), lizard-like inhabitant of warm, shallow coastal waters (*5*). In pachypleurosaurids, aquatic adaptation had not progressed as far as in plesiosaurs and ichthyosaurs, and the animals clearly were still able to leave the water (*3*).

Of the 97 prepared skeletons of *Neusticosaurus* sp., 24 are juveniles and furnish a complete growth series (Figs. 2 and 3). This large sample made sexing (sex A and B) and recognition of sexual maturity possible. The very homogeneous sample comes from a narrow stratigraphic interval and is treated as representing a single population. The

Paläontologisches Institut und Museum, Universität Zürich, Künstlergasse 16, CH-8006 Zurich, Switzerland.

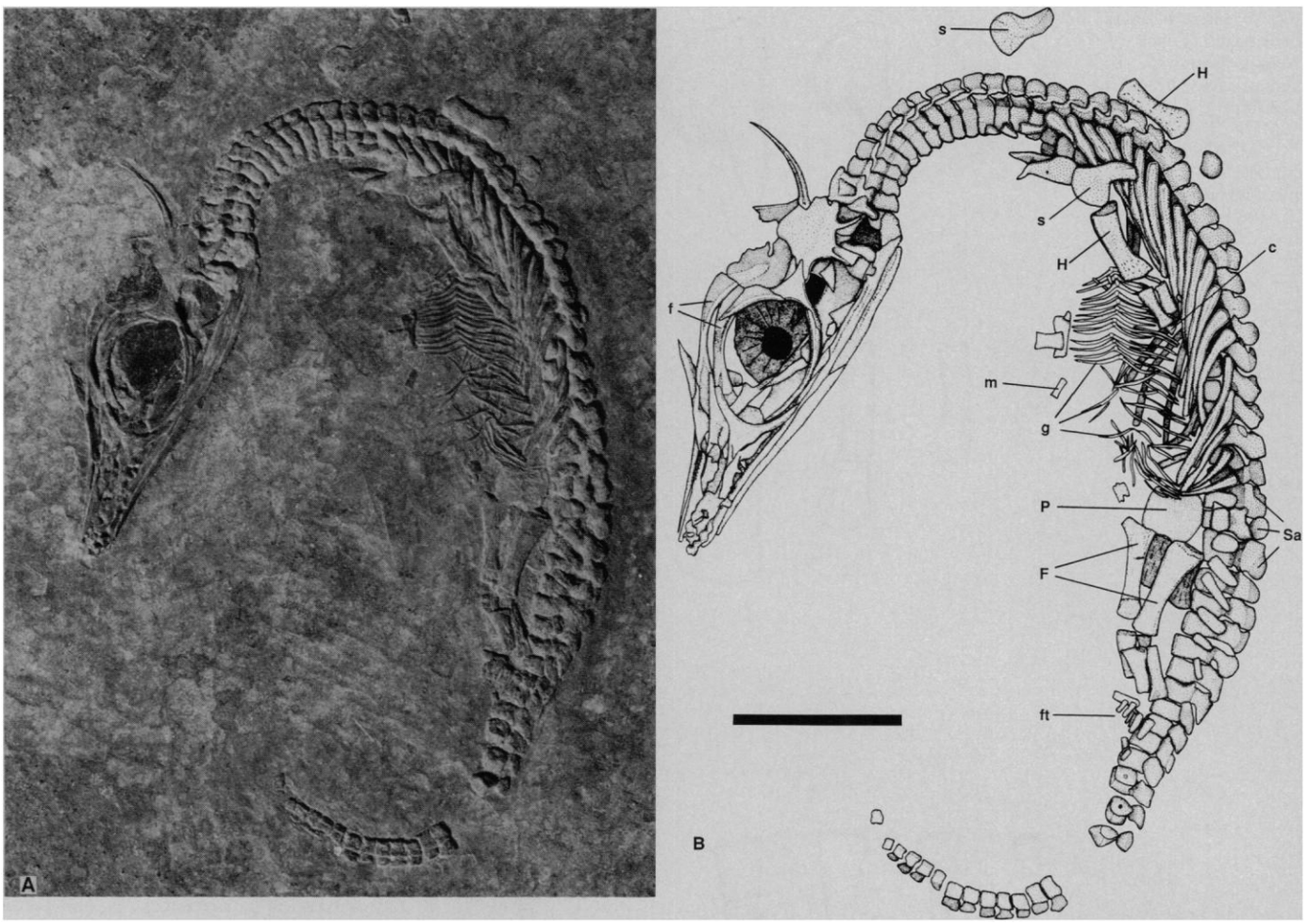

Fig. 1. Embryo of *Neusticosaurus* sp., PIMUZ T 3705: (**A**) photograph of skeleton; (**B**) drawing of skeleton. Abbreviations for bones: c, carpal; F, femur; f, frontal; ft, foot; g, gastralia; H, humerus; m, metacarpal; P, pubis; s, scapula; and Sa, sacral vertebrae. Scale bar, 5 mm.

smallest specimen (PIMUZ T 3705, Fig. 1) is an embryo a few stages before hatching. Two independent lines of evidence support this conclusion: the morphology of the specimen and its absolute and relative size.

Neusticosaurus skeletons are always preserved in dorsoventral view, with two exceptions: PIMUZ T 3705 and PIMUZ T 3396 (adult) which lie on their sides. PIMUZ T 3705 (Fig. 1) is curled up with the head close to the tail, a unique pose for *Neusticosaurus* but a typical position for vertebrate embryos. The skull is of relatively enormous size, 76% of trunk length (glenoid-acetabulum distance) with very large orbits. This value is only 40 to 50% in adults (Fig. 2). In the poorly ossified skull, the frontal bones are unfused and disarticulated. They are fused in the adult. Only a few teeth are present. The entire vertebral column, but especially the neck, is compressed anteroposteriorly with very short but high vertebrae. Only two-thirds of the tail vertebrae and only five (of eight) caudal ribs are present. The tail reaches only 170% of trunk length, whereas the tail in juveniles reaches

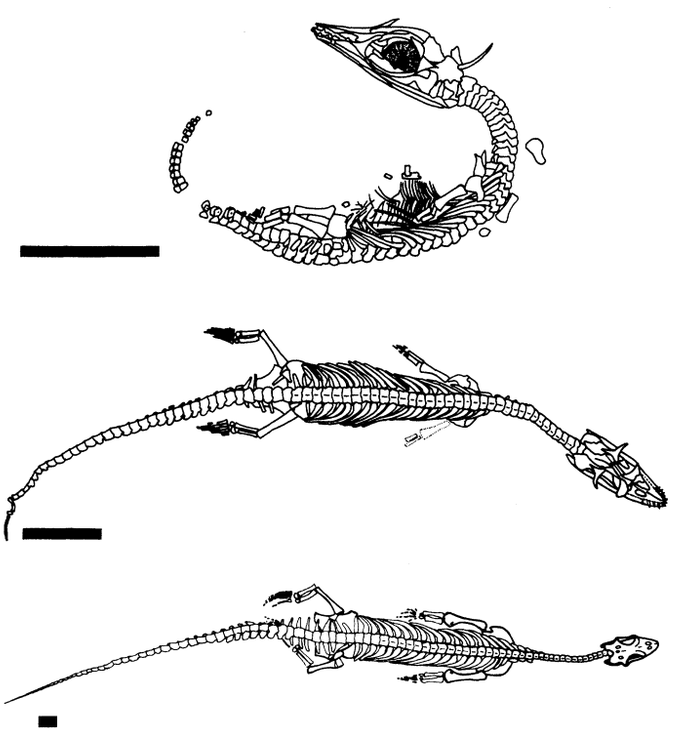

Fig. 2. Growth series of three skeletons of *Neusticosaurus* sp. drawn to the same body length. PIMUZ T 3705 is the embryo, PIMUZ T 3408 is a small juvenile, and PIMUZ T 3393 is a large adult of sex B. Note relative size of skull and relative humerus and tail length. Scale bars, 1 cm each.

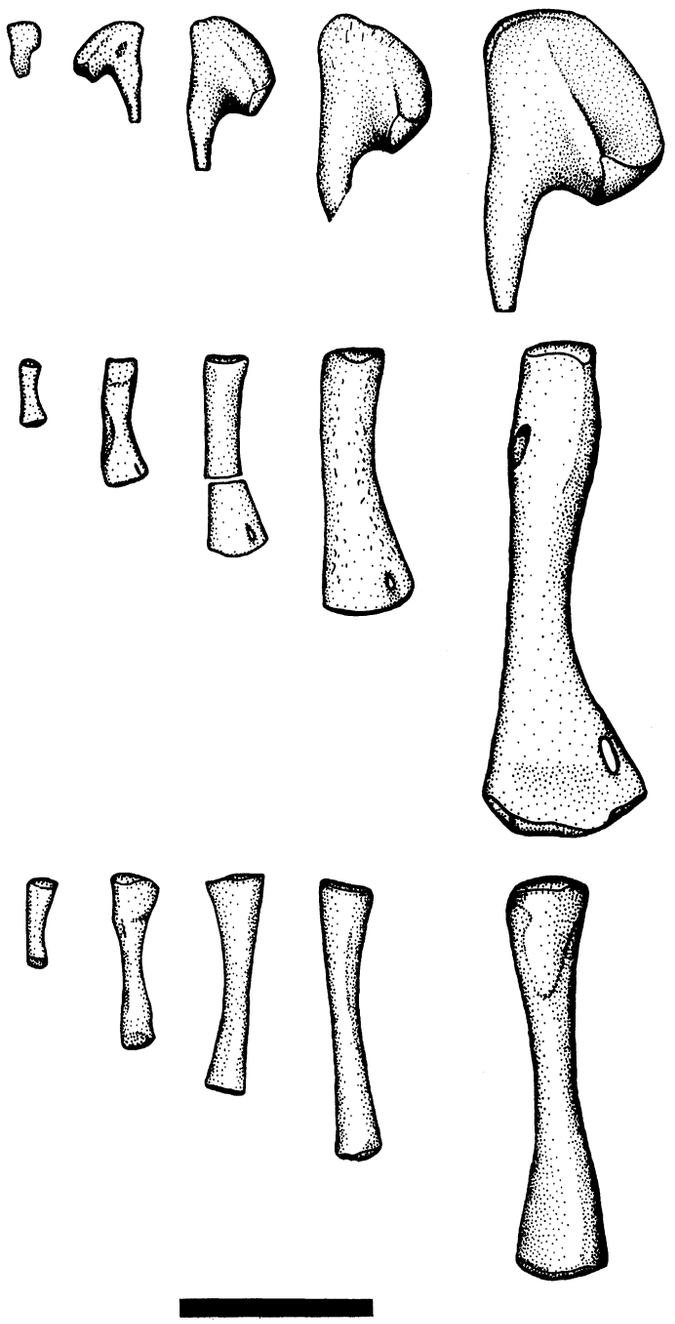

Fig. 3. Growth series of selected bones of *Neusticosaurus* sp. in ventral view. PIMUZ T 3705 is the embryo, PIMUZ T 3789, PIMUZ T 4290, and PIMUZ T 3389 are juveniles, whereas PIMUZ T 3403 is a small adult of sex B. All bones are from the right side of the body with the exception of the scapula of PIMUZ T 3789 and the femur of PIMUZ T 4290. Note the shape differences in the scapulae and the proportional differences between the humeri and femora. Scale bar, 5 mm.

about 190% and that of adults 200 to 220% of trunk length (Fig. 2). In the shoulder girdle, the interclavicle is not yet ossified, and the scapulae differ greatly in shape from the adult (Fig. 3) as do the bones in the pelvic girdle. Humerus and femur (Fig. 3) are featureless rods with slightly expanded, poorly ossified terminations. The humerus is much shorter than the femur; 75% of the femur instead of 110% in adults of sex A or 130% in adults of sex B (Figs. 2 and 3). The manus is unossified except for one carpal and one metacarpal bone. The foot shows no tarsals but some metatarsals and possible proximal phalanges. Surprisingly for the poor ossification of the skeleton, the gastralia are fully developed.

The second smallest specimen (PIMUZ T 3789, body length 94 mm) is a hatchling which is ossified close to the adult level, only the proportions are juvenile (Fig. 3). This is the condition observed in the (rare) fossil (*8*) and modern reptile hatchlings (*9*).

Studies about hatchling to adult size ratios in modern lizards and crocodilians by Currie and Carroll (*10*), and in all modern reptiles except *Sphenodon* by Andrews (*11*), can be used to predict the overall body length (*10*) or snout-vent length (*11*) of hatchlings. The hatchling-adult ratio for *Sphenodon* (*12*) is consistent with the predictions and data of both Currie and Carroll (*10*) and Andrews (*11*). The results can as well be applied to extinct reptiles of small to moderate size assuming they had the same level of metabolism as modern forms (*10*). Only the lizard, snake, and crocodile data were used because the turtle *Bauplan* is too different from the pachypleurosaurid proportions.

The mean adult body length of *Neusticosaurus* sp. is 240 mm, and the mean adult snout-vent length is 155 mm. The Currie and Carroll (*10*) formula predicts a hatchling of 71-mm overall body length (29% of adult body size). Specimen T 3705 is 51 mm long (21% of adult). Andrews' (*11*) data predict a hatchling snout-vent length of 48 mm (31% of adult) based on lizards, 59 mm (39% of adult) based on snakes, or 72 mm (46% of adult) based on crocodilians. The snout-vent length of T 3705 is 34 mm (22% of adult). The embryo therefore reached only about two-thirds of hatchling size before death.

It is unclear if pachypleurosaurs were live-bearing or egg-laying. Ovipary (hatching from an egg) is supported by two lines of circumstantial evidence. First, despite the great wealth of sexed pachypleurosaurid material, no gravid female has ever been found, unlike in *Mixosaurus*, a primitive ichthyosaur from the same locality. The embryo was not associated with any other skeleton. Second, pachypleurosaurids could venture on land (*3*) and were therefore not limited to vivipary as were the most highly adapted marine reptiles, ichthyosaurs (*1*), and possibly mosasaurs (*13*). Today, even such highly aquatic animals as marine turtles still retain the egg-laying habit.

On the other hand, vivipary (live birth), that is, interpretation of the specimen as an aborted embryo, is supported by the sediments that are fully marine and suggest a coast several kilometers away. It is not clear how a well-incubated amniote egg, which must have been laid on dry land, could have been transported so far out into the sea. However, paleogeography of the Monte San Giorgio in Early Ladinian times remains poorly understood.

The curled position of the embryo and the lack of eggshell remains are ambiguous evidence. A calcified or uncalcified eggshell had a small preservation potential in the bituminous shales of Monte San Giorgio. Even though bone preservation is good, soft part preservation is extremely rare as are calcareous invertebrate fossils.

REFERENCES AND NOTES

1. A. S. Romer, *Vertebrate Paleontology* (Univ. of Chicago Press, Chicago, ed. 2, 1966), p. 119.
2. P. J. Currie, *Soc. Vert. Paleontol. News Bull.* (October 1987), p. 10; *J. Vert. Palentol.* 7, 15a (1987).
3. R. L. Carroll and P. Gaskill, *Philos. Trans. R. Soc. London* **B309**, 348 (1985).
4. H. Rieber and L. Sorbini, *Middle Triassic Bituminous*

Shales of Monte San Giorgio (Tessin, Switzerland), Excursion 11A (First International Congress of Paleoecology, Lyon, 1983).
5. E. Kuhn-Schnyder, *Neujahrsblatt Naturf. Ges. Zürich* **176**, 102 (1974).
6. K. F. Hirsch, *J. Paleontol.* **53**, 1068 (1979).
7. A. H. Müller, *Lehrbuch der Paläozoologie, Allgemeine Grundlagen* (Fischer, Jena, ed. 3, 1976), vol. 1, p. 313.
8. J. R. Horner and R. Makela, *Nature (London)* **282**, 297 (1979).
9. C. Gans *et al.*, Eds., *Biology of the Reptilia, Development A* (Wiley, New York, 1985), vol. 14.
10. P. J. Currie and R. L. Carroll, *J. Vert. Paleontol.* **4**, 76 (1984).
11. R. M. Andrews, in *Biology of the Reptilia, Physiology D*, C. Gans and H. F. Pough, Eds. (Academic Press, London, 1982), vol. 13, pp. 280–282.
12. L. A. Moffat, in (*9*), pp. 496–499.
13. J. L. Dobie, D. R. Womochel, G. L. Bell, *J. Vert. Paleontol.* **4**, 197 (1986).
14. I thank O. Rieppel for encouragement and assistance and for improving the manuscript along with C. T. Gee and H. Rieber and H. Lanz for the photographic work.

14 September 1987; accepted 8 December 1987

Mesoderm Induction in Amphibians: The Role of TGF-β2–Like Factors

FRÉDÉRIC ROSA, ANITA B. ROBERTS, DAVID DANIELPOUR, LINDA L. DART, MICHAEL B. SPORN, IGOR B. DAWID

Mesoderm induction in the amphibian embryo can be studied by exposing animal region explants (destined to become ectoderm) to appropriate stimuli and assaying the appearance of mesodermal products like α-actin messenger RNA. Transforming growth factor β2 (TGF-β2), but not TGF-β1, was active in α-actin induction, while addition of fibroblast growth factor had a small synergistic effect. Medium conditioned by *Xenopus* XTC cells (XTC-CM), known to have powerful mesoderm-inducing activity, was shown to contain TGF-β–like activity as measured by a radioreceptor binding assay, colony formation in NRK cells, and growth inhibition in CCL64 cells. The activity of XTC-CM in mesoderm induction and in growth inhibition of CCL64 cells was inhibited partially by antibodies to TGF-β2 but not by antibodies to TGF-β1. Thus, a TGF-β2–like molecule may be involved in mesoderm induction.

INDUCTIVE INTERACTIONS ARE CRITICAL to the elaboration of the body plan of all vertebrate embryos, as studied most extensively in amphibians. The earliest known induction concerns the establishment of the mesoderm (*1*). In normal embryogenesis the mesoderm develops mostly from cells that occupy a torus around the equator of the blastula, while cells from the animal hemisphere ("animal caps") primarily generate ectodermal derivatives (*1, 2*). Only ectodermal differentiation occurs after culture of animal caps derived from blastulae; mesodermal derivatives arise when animal caps are cultured in contact with vegetal tissue, implying an inductive interaction in mesoderm differentiation (*1*). Such interactions almost certainly also occur in normal embryogenesis (*3, 4*).

As shown by Smith (*5*) medium conditioned by the *Xenopus* XTC cell line (XTC-CM) is able to induce animal caps to form various mesodermal derivatives including muscle. Subsequently, Slack *et al.* (*6*) reported that fibroblast growth factor (FGF) has inducing activity, yielding various products including muscle (a dorsal mesodermal tissue), but primarily inducing ventral mesoderm, such as blood cells. Kimelman and Kirschner (*7*) reported that transforming growth factor β (TGF-β) potentiates the effect of FGF in inducing α-actin (indicating formation of muscle tissue).

TGF-β is known to occur in two related forms (*8, 9*). To further study the relationship of these factors to mesoderm induction we incubated animal explants from *Xenopus laevis* blastula embryos in medium containing TGF-β1 or TGF-β2 (*10*). TGF-β2 was found to induce mesoderm according to the following two criteria. In the presence of TGF-β2, animal explants formed elongated structures (Fig. 1A) reminiscent of mesodermal derivatives of the marginal zone and similar to those obtained with the mesoderm-inducing XTC-CM (Fig. 1B) (*5*). Further, TGF-β2 induced the expression of α-actin messenger RNA (mRNA) in the explants (Fig. 2A). During *Xenopus* embryogenesis, muscle-specific α-actin mRNA accumulates exclusively in the somites from stage 13 to 14 onward, providing the earliest known molecular marker for the differentiation of muscle (*11*). The lowest concentration of TGF-β2 that induced detectable α-actin mRNA varied from 3 to 12 ng/ml in different experiments; mRNA levels continued to increase until the TGF-β2 concentration was raised to about 200 ng/ml. The maximal level of α-actin mRNA induced by TGF-β2 was significantly lower than that found in heat- or acid-activated XTC-CM–treated animal explants (Fig. 2A). In agreement with other reports (*6, 7*), we found that TGF-β1 did not exhibit detectable mesoderm-inducing activity (Fig. 2A).

FGF exhibits weak muscle inducing activity (*6*), and it has been reported that this activity is potentiated by TGF-β (*7*). We tested α-actin induction by combinations of FGF with TGF-β1 or TGF-β2. TGF-β2 and FGF induced α-actin mRNA effectively, but the maximal level of mRNA obtained was the same as with TGF-β2 alone; the only effect of combining the two factors was a shift in the TGF-β2 dose response (Fig. 2B). In contrast, a moderate and somewhat variable enhancement was seen in the interaction between FGF and TGF-β1: the combination of these factors led to between two and three times higher α-actin induction than FGF alone, while TGF-β1 alone had no effect (Fig. 2, A and B).

Since XTC-CM (*5*) is a homologous material and has the highest inducing ability in these experiments, we wished to test whether the activity in XTC-CM and TGF-β2 (Figs. 1 and 2) might be related. Two approaches were taken. First, XTC-CM was assayed for TGF-β–like activity by several different methods; these assays do not differentiate between TGF-β1 and -β2 . Second, polyclonal blocking antibodies specific against TGF-β1 or -β2 were tested for their ability to inhibit both the TGF-β–like activity as well as the mesoderm-inducing activity of XTC-CM.

By means of a competitive radioreceptor binding assay (*12*), it could be shown that XTC-CM competed weakly for the binding of ^{125}I-labeled TGF-β1 (Fig. 3A). Pretreatment of XTC-CM with acid, a treatment known to activate latent TGF-β (*13*), resulted in a ninefold enhancement of the competing activity of XTC-CM; acid-treated XTC-CM was estimated to contain 220 p*M* (5 ng/ml) TGF-β activity, by comparison to the standard (Fig. 3A). Although purified TGF-β is intrinsically active, TGF-β secreted by many different human or rodent cell lines is in a latent form which is unable to bind to

F. Rosa and I. B. Dawid, Laboratory of Molecular Genetics, National Institute of Child Health and Human Development, National Institutes of Health, Bethesda, MD 20892.
A. B. Roberts, D. Danielpour, L. L. Dart, M. B. Sporn, Laboratory of Chemoprevention, Division of Cancer Etiology, National Cancer Institute, National Institutes of Health, Bethesda, MD 20892.